PHYSICAL REVIEW B **81**, 094524 (2010)

Multiple electronic transitions and superconductivity in Pd_xTiSe_2

E. Morosan,[1,*] K. E. Wagner,[2] Liang L. Zhao,[1] Y. Hor,[2] A. J. Williams,[2] J. Tao,[3] Y. Zhu,[3] and R. J. Cava[2]
[1]*Department of Physics and Astronomy, Rice University, Houston, Texas 77005, USA*
[2]*Department of Chemistry, Princeton University, Princeton, New Jersey 08540, USA*
[3]*Condensed Matter Physics and Materials Science, Brookhaven National Laboratory, Upton, New York 11973, USA*
(Received 4 January 2010; revised manuscript received 13 February 2010; published 26 March 2010)

We report the synthesis and characterization of Pd_xTiSe_2 via magnetization, resistivity, specific heat measurements, and low-temperature electron diffraction. At very low levels of intercalation, near $Pd_{0.01}TiSe_2$, the commensurate charge density wave transition in the $TiSe_2$ parent compound near 220 K becomes substantially stronger; a distinct transition to a more resistive state is seen at about 80 K. Originally semimetallic, $TiSe_2$ becomes an insulator at low temperatures for $0.01 \leq x \leq 0.06$ in Pd_xTiSe_2. Increasing Pd intercalation beyond this level begins to suppress the insulating behavior until a 2 K superconductor is found in the narrow composition range of $0.11 \leq x \leq 0.12$. Beyond $x=0.12$, a normal metallic state (down to 0.3 K) is induced.

DOI: 10.1103/PhysRevB.81.094524 PACS number(s): 71.45.Lr, 71.30.+h, 74.25.Dw

The MX_2 layered dichalcogenides display a wealth of electronic properties,[1] from insulators (HfS_2) and semiconductors (MoS_2) to semimetals (WTe_2 and TcS_2) and metals (NbS_2 and VSe_2). Given their layered structure, charge density wave (CDW) transitions often coexist with superconductivity in these materials and chemical doping[2,3] or pressure[4–6] have often been employed to study the competition between the two correlated electronic states. It is frequently observed that external perturbation destabilizes CDWs and favors an increase in the critical temperature of the superconductivity.

$TiSe_2$ is unusual as both an undoped compound[7,8] and upon Cu intercalation.[9] For $TiSe_2$ only the 1T polytype is known, a structure with a single layer of edge-sharing $TiSe_6$ octahedra. The normal state of $TiSe_2$ is currently believed to be either a semimetal[6–8,10–15] or a semiconductor[16–18] with a small indirect gap. Below ~220 K, a CDW transition occurs, into a state with a commensurate (2a,2a,2c) wave vector and no intermediate incommensurate phase.[7,10,19] The origin of the CDW remains controversial, but the consensus is that it is not driven by Fermi surface nesting. No superconductivity has been observed in this compound down to 0.3 K. However, with Cu doping to form Cu_xTiSe_2 (Ref. 9) the CDW transition is continuously suppressed, continuous evolution to metallic behavior is observed, and superconductivity emerges at around $x=0.04$. The superconducting transition temperature T_c does not evolve monotonically with x; instead, a classic dome of superconductivity is observed, peaking at $T_c=4.15$ K for $x=0.08$; superconductivity is observed up to the solubility limit $x=0.11$ in Cu_xTiSe_2. Monovalent nonmagnetic Cu ions act as an n-type dopant, which is manifested in the continuous increase in the metallicity of Cu_xTiSe_2 and the negative Seebeck coefficient,[9] and seen in the Fermi surface.[20]

In this paper, we report unexpected, more complex electronic behavior in the analogous Pd_xTiSe_2 system. Like Cu, Pd is a non-magnetic dopant, with one less valence electron per dopant atom than Cu. The system displays four different electronic states at low temperatures as the level of Pd doping is varied over the range of the solid solution, which exists for Pd_xTiSe_2 for $0.00 \leq x \leq 0.18$. Very small levels of Pd doping increase the strength of the commensurate CDW in $TiSe_2$, with a distinct second transition near 80 K for $x \approx 0.01$ leading to more insulating behavior at low temperatures. Although multiple CDW transitions have been observed previously in several compounds,[21–25] to our knowledge Pd_xTiSe_2 is the first system where a second electronic transition follows upon further cooling a commensurate high-T CDW. Insulator-like behavior is observed for Pd_xTiSe_2 for $0.01 \leq x \leq 0.06$. As x increases further, the CDW transition is driven down in temperature and Pd_xTiSe_2 becomes more metallic until superconductivity is observed for a very narrow concentration range ($0.11 < x < 0.12$). Beyond this doping level, for $0.14 < x < 0.18$, the system changes its low-temperature state again, becoming a normal metal down to 0.3 K.

Polycrystalline samples of Pd_xTiSe_2 for $x=0$, 0.01, 0.02, 0.03, 0.04, 0.06, 0.08, 0.10, 0.11, 0.12, 0.14, 0.16, and 0.18 were synthesized via solid state reaction. Stoichiometric amounts of Pd, Ti, and Se in powder form were first heated up to 650 °C overnight and then air quenched. Next, the dark purple powders were pressed into pellets and annealed at 650 °C for another day, followed by air quenching to room temperature. Powder x-ray diffraction data were recorded on a Bruker D8 diffractometer, using Cu Kα radiation and a graphite diffracted beam monochromator. These measurements confirmed the 1T-$TiSe_2$ structure type for the Pd_xTiSe_2 series, with both the a and c lattice parameters increasing with increasing x [Fig. 1(a)]. Quantitative refinement of the x-ray data for $Pd_{0.18}TiSe_2$ [Fig. 1(b)] indicates that Pd is intercalated into the octahedral sites in the Van der Waals gaps between the $TiSe_2$ layers.

Although the same structural behavior was observed in Cu_xTiSe_2,[9] its monotonic increase in the lattice parameters was accompanied by a continuous increase in metallic character. Strikingly, Pd intercalation has a substantively different effect on the transport properties of $TiSe_2$. As illustrated in Fig. 2, the smallest amount of Pd doping ($x=0.01$) increases the low-temperature resistivity of $TiSe_2$ by nearly two orders of magnitude. For a limited Pd doping range ($0.01 \leq x \leq 0.06$), Pd_xTiSe_2 behaves like an insulator, with the low-temperature resistivity nearly one thousand times larger than that at room temperature.

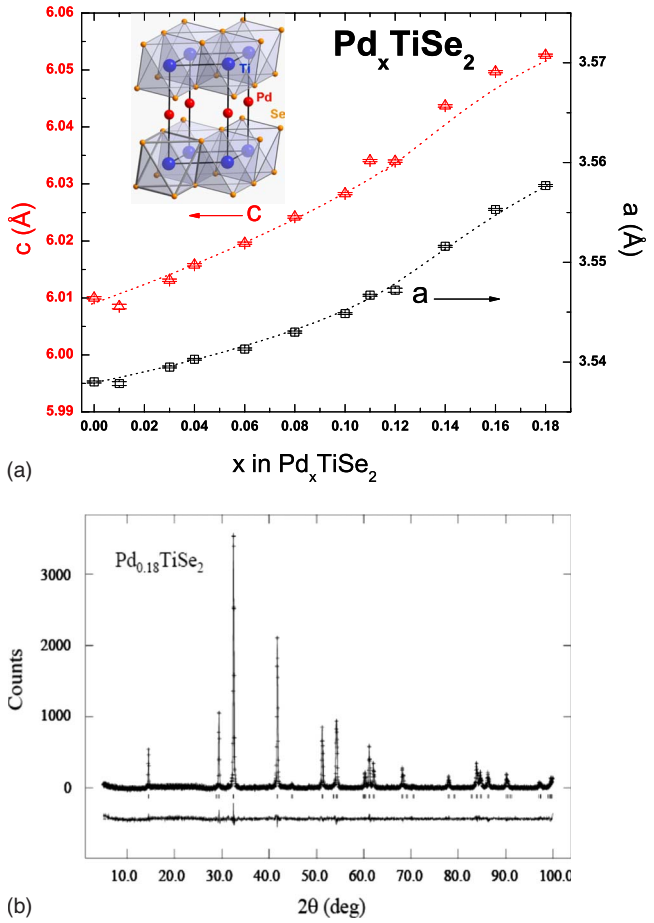

FIG. 1. (Color online) (a) Lattice parameters a (right axis) and c (left axis) as a function of x in Pd_xTiSe_2, with the crystal structure shown in the inset. (b) Powder x-ray diffraction data and refinement for $Pd_{0.18}TiSe_2$, confirming the 1T polytype of the Pd-intercalated $TiSe_2$ compounds.

In order to understand the change in the resistivity of Pd_xTiSe_2, we have to first consider the unusual $\rho(T)$ for the parent compound: a local maximum that is observed around 150 K in $TiSe_2$ (black curve in Fig. 2) has been attributed to the partial gapping of the Fermi surface at the CDW transition.[7] This first yields the increase in $\rho(T)$ upon cooling, followed by a decrease of the resistivity at low enough temperatures as the systems recovers its metallic character due to the presence of ungaped portions of the Fermi surface. We surmise that, with the intercalation of small amounts of Pd, the Fermi surface is more fully gapped and the CDW becomes stronger. This results in a higher resistivity at low temperature in the Pd-doped case than for pure $TiSe_2$ (Fig. 2). The additional inflexion below 80 K in the resistivity of the $x=0.01$ sample, more clearly seen in the derivatives $d\rho/dT$ (red curve, Fig. 2 inset) marks the transition to this stronger CDW state. The strength of the enhanced CDW state is sufficiently large that only for $x \geq 0.11$ does the resistivity of Pd_xTiSe_2 drop for the whole temperature range below 300 K, in contrast to the case for Cu_xTiSe_2, where continuously dropping resistivity is seen for $x \geq 0.03$.[9] Superconductivity emerges for a narrow Pd concentration ($0.11 \leq x \leq 0.12$) in Pd_xTiSe_2 as shown in Fig. 3, albeit with a

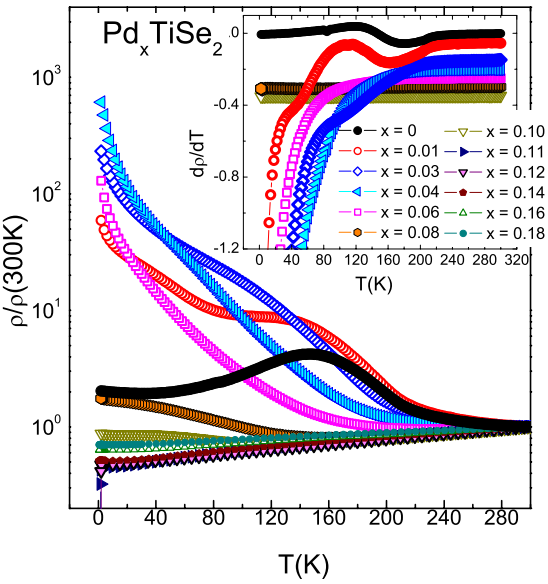

FIG. 2. (Color online) Temperature-dependent resistivity data (scaled at 300 K) for Pd_xTiSe_2 on a semilog plot, with the derivatives $d\rho/dT$ shown in the inset.

smaller critical temperature ($T_c \leq 2$ K) than in the Cu-doped case.

The temperature-dependent magnetization $M(T)/H$ (Fig. 4) is less sensitive to the second electronic transition at low x, but it does show signatures of the initial CDW transition: in the undoped case (black symbols, Fig. 4) a drop in the magnetization below 220 K is associated with the removal of states at the Fermi level as $TiSe_2$ enters the CDW state. Pd doping slowly suppresses the CDW transition temperature in Pd_xTiSe_2 for low x values, such that T_{CDW} drops to around 160 K for $x=0.06$. Higher doping levels result in a nearly composition-independent magnetization. The additional gapping of the Fermi surface below 80 K is obscured in the magnetization data by a low-temperature Curie-Weiss-like tail. This is likely due to a small local moment induced by Pd doping, with a corresponding magnetic moment smaller than 0.15 μ_B/F.U. and independent of composition for $0 \leq x \leq 0.18$. Vertical arrows in Fig. 4 indicate the extreme CDW

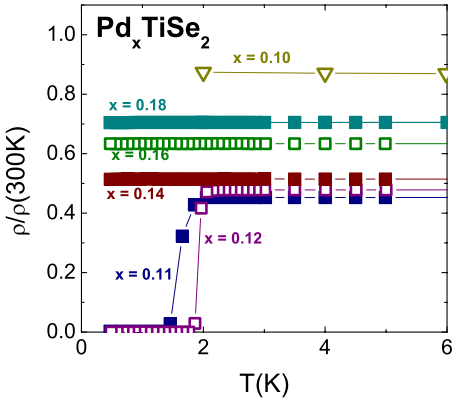

FIG. 3. (Color online) Low-temperature $\rho(T)$ data for $0.10 \leq x \leq 0.18$ for Pd_xTiSe_2, showing the superconducting transitions for $x=0.11$ and 0.12.

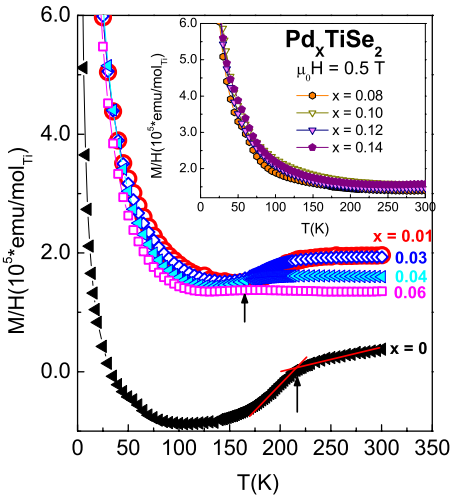

FIG. 4. (Color online) μ_0H=0.5 T temperature-dependent magnetic susceptibility data for Pd_xTiSe_2, $0 \leq x \leq 0.06$, indicating a drop in susceptibility associated with the CDW transition. Vertical arrows mark the extreme T_{CDW} values. Inset: magnetic susceptibility data for $0.08 \leq x \leq 0.14$, where the CDW transition is no longer visible.

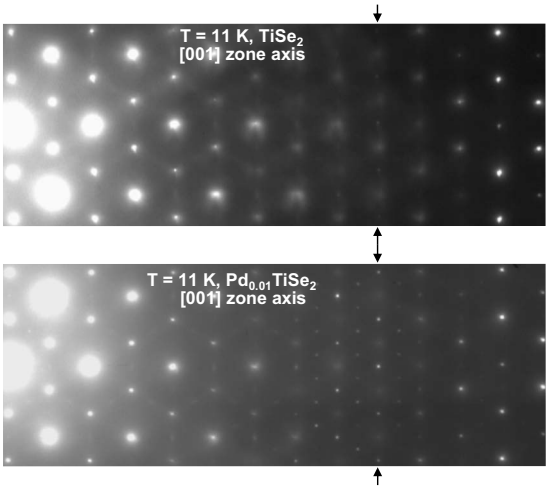

FIG. 5. T=11 K electron diffraction patterns of the (a) $TiSe_2$ and (b) $Pd_{0.01}TiSe_2$ reciprocal lattices. The crystals are tilted away from the (001) zone axis, to show the superreflections in higher-order Laue zones. The diffraction pattern in (a) shows much weaker superlattice reflections compared to the analogous ones for the doped sample (b).

transition temperatures, detected in M(T) for x=0 and 0.06 respectively. Due to the same Curie-Weiss increase in the low-temperature data, the CDW transition can no longer be identified in M(T) for doping levels higher than x=0.06 (inset, Fig. 4), for which the magnetization is nearly composition independent.

To directly probe the nature of the low-temperature CDW state, electron diffraction experiments were performed at 11 K on pure $TiSe_2$ and doped $Pd_{0.01}TiSe_2$ (Fig. 5) using the JEOL 3000F transmission electron microscope equipped with a Gatan liquid-helium cooling stage. The electron diffraction patterns were recorded on 20 bit Ditabis imaging plates for digital analysis. Consistent with the previous reports on the (2a,2a,2c) commensurate CDW in $TiSe_2$ (Ref. 7) and Cu_xTiSe_2,[9] our measurements show the presence of (1/2,1/2,1/2)-type superreflections at low temperatures in both pure $TiSe_2$ [Fig. 5(a)] and in $Pd_{0.01}TiSe_2$ [Fig. 5(b)]. Remarkable, however, is that, at T=11 K, the superstructure reflections are much stronger in $Pd_{0.01}TiSe_2$ than they are in $TiSe_2$. This indicates that low levels of Pd doping increase the strength of the CDW at low temperatures compared to $TiSe_2$. This much more stable CDW state in Pd_xTiSe_2 is harder to destabilize on doping than was the case in Cu_xTiSe_2.[9] The much stronger and more stable CDW in Pd_xTiSe_2 explains the insulating electronic state for x =0.01–0.06, and that higher doping levels (x=0.11–0.12) are necessary to induce the CDW-to-superconductivity transition. This stronger CDW stability may also explain why T_c is lower for the Pd-doped case, as the interactions leading to the insulating state are not fully suppressed.

The measured room-temperature resistivity values, between 1 and 4 mΩ cm, do not show a systematic trend with x in the polycrystalline samples, but the scaled resistivity values ρ(300 K)/ρ(4 K), nicely trace the systematic behavior in the series, as seen in Fig. 6. As soon as a small amount (x=0.01) of Pd is intercalated into $TiSe_2$, ρ(300 K)/ρ(4 K) decreases abruptly, and is continuously suppressed in the doping range x=0.01–0.03. Pd_xTiSe_2 becomes more and more insulating as the low-temperature electronic transition becomes stronger and stronger. This is in stark contrast to Cu-doping of $TiSe_2$ (Ref. 9) where increasing Cu content continuously enhances the metallicity, and thus increases the ratio ρ(300 K)/ρ(4 K). For much higher x, the material becomes more metallic. This is seen in the ratio ρ(300 K)/ρ(4 K), which features a sharp increase to a maximum at x=0.11 (Fig. 6). Superconductivity occurs exactly after this sharp increase in metallicity, and then disappears with further doping. The similarities between Cu and Pd doping of $TiSe_2$ are thus restored for intermediate

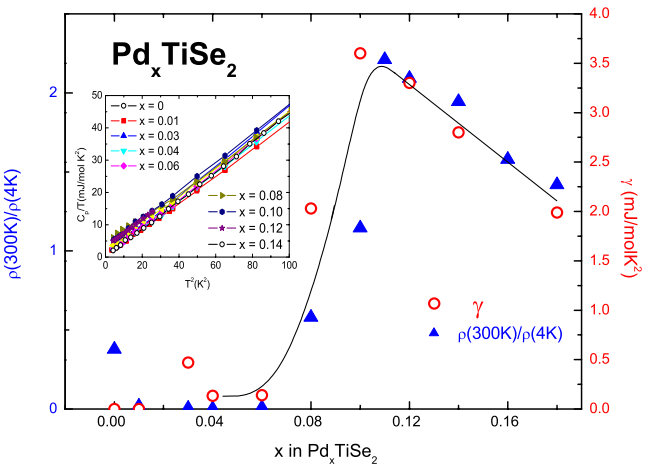

FIG. 6. (Color online) ρ(300 K)/ρ(4 K) (left axis) and electronic specific-heat coefficient γ (right axis) as a function of x in Pd_xTiSe_2. The line is a guide to the eye, emphasizing the increase in both quantities at intermediate compositions, and their nearly linear decrease beyond the superconducting state (for x>0.12).

dopant concentrations, but at high x values the two sets of compounds once again show different transport properties: in the former case, the compounds remain good metals, with the ratio $\rho(300\ \mathrm{K})/\rho(4\ \mathrm{K})$ continuously increasing up to the solubility limit $x=0.11$ in Cu_xTiSe_2. In the current case, beyond the superconducting state, the low-temperature resistivity of Pd_xTiSe_2 increases slowly with x and consequently the ratio $\rho(300\ \mathrm{K})/\rho(4\ \mathrm{K})$ has a downward trend (Fig. 6).

The electronic specific heat coefficients γ for the Pd_xTiSe_2 series are also shown in Fig. 6 (open circles). γ has a strikingly similar dependence on x as $\rho(300\ \mathrm{K})/\rho(4\ \mathrm{K})$: it remains nearly unchanged ($\sim 1\ \mathrm{mJ/mol\ K^2}$) throughout the insulating regime ($x \leq 0.06$) and rapidly increases up to $\sim 4\ \mathrm{mJ/mol\ K^2}$ in the superconducting regime. For the normal metal, where any superconductivity, if present, is suppressed below 0.3 K ($x>0.12$), a decrease in γ qualitatively follows the decrease in the resistivity ratio. These results suggest that the dramatic behavior of the composition dependent resistivities in Pd_xTiSe_2 up to the superconducting compositions $x=0.11-0.12$ primarily reflect changes in the number of carriers present due to the Pd doping. In contrast, and consistent with the continuously increasing metallicity, the Cu_xTiSe_2 series shows a continuous increase in γ in the composition range up to $x=0.11$.

It is unusual that tuning using a single control parameter, in this case Pd doping of $TiSe_2$, spans such a broad spectrum of electronic properties. This is reflected in the T-x phase diagram in Fig. 7: from a semiconducting or semimetal state in the parent $TiSe_2$ compound this system transforms into a commensurate CDW state below 220 K, then into a low temperature more insulating state for low Pd content ($x \leq 0.06$), then to a superconducting state at low temperatures for intermediate compositions ($0.11 \leq x \leq 0.12$), and finally to normal metallic state for $x>0.12$. Multiple CDW transitions have previously been observed in transition metal chalcogenides $NbSe_3$,[21] 4Hb-TaS_2,[22] in tungsten bronzes $W_{12}P_4O_{44}$ and $W_{14}P_4O_{50}$,[23] in the R=Ho, Er, and Tm members of the $R_5Ir_4Si_{10}$ series[24] and more recently in the RTe_3 compounds (R=Ho, Er, and Tm).[25] The observation of a second CDW transition in all of these systems can be attributed to nesting of different regions in the Fermi surface. Pd_xTiSe_2 is novel with regard to the observation of a second transition within the CDW state since the above scenarios do not apply: the CDW in undoped $TiSe_2$ is commensurate and its wave vector is preserved with Pd doping. The stability of the high-T CDW, viewed through its transition temperature, is unaffected by Pd doping in the low composition range where the additional low-T transition to the low-temperature insulator is observed ($x \leq 0.03$); the high-T CDW transition temperature starts decreasing only for $x>0.03$. Optical spectroscopy studies performed on the parent compound, $TiSe_2$ (Refs. 1 and 14) indicate that parts of the Fermi surface remain ungaped after the 220 K CDW transition, leaving the compound in a semimetallic state even at low temperatures. It may be that at the lowest Pd concentrations the insulating behavior is induced because the Fermi surface becomes more fully gapped, either by removing portions that were not initially gapped in pure $TiSe_2$ or by increasing the difference in energy between filled and empty states.

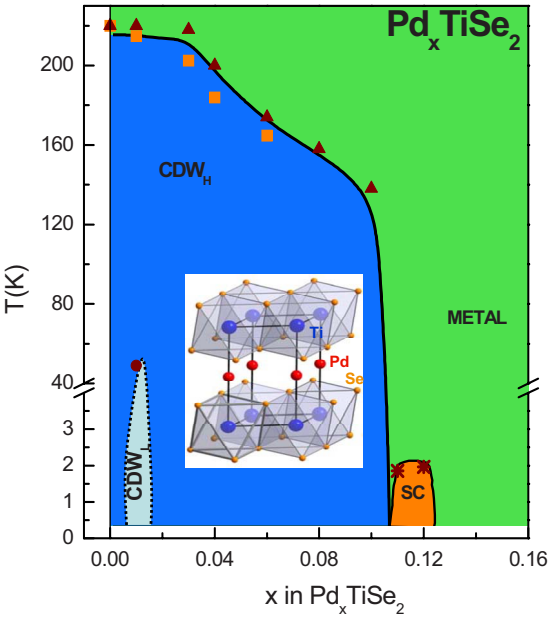

FIG. 7. (Color online) Electronic phase diagram for Pd_xTiSe_2. Brown and orange points are determined from resistivity and magnetization data respectively. Solid lines are shown for the high-T CDW (CDW_H) and superconducting phase boundaries. The dotted lines for the second electronic transition within the CDW phase (CDW_L) are hypothetical phase boundaries where the transitions are not visible in the data. Inset: the crystal structure of Pd_xTiSe_2.

Both Cu and Pd intercalation of $TiSe_2$ ultimately induce superconductivity; for $x=0.04-0.11$ and a maximum T_c of 4.15 K in Cu_xTiSe_2, and for $x=0.11-0.12$ and $T_c \approx 2$ K in Pd_xTiSe_2, but the evolution of the electronic phases present at low temperatures is much more complex in the Pd-doped case. It is tempting to attribute this to the more ambiguous character of the electronic state of the Pd intercalant. The electron configuration of Cu, $3d^{10}4s^1$, indicates that in covalent compounds like Cu_xTiSe_2 the high energy Cu 4s state will become empty, yielding its one electron for doping the $TiSe_2$ layer. This scenario is verified by the angle-resolved photoemission spectroscopy characterization of the superconducting phase.[20] For Pd, the electron configuration $4d^{10}5s^0$ means that if the Pd 4d states remain completely filled in Pd_xTiSe_2, then no electrons are nominally available for doping the $TiSe_2$ layer. This type of situation is seen for example in half-Heusler phases such as LuPdSb.[27] Thus, the Pd intercalation of $TiSe_2$ is particularly interesting from an electronic perspective—we cannot determine without further study whether the insulating, then superconducting, then metallic states are induced due to electron concentration changes, bandwidth changes, or disorder effects. Finally, Raman scattering studies have indicated that a quantum critical phase transition is present within the superconducting composition region in Cu_xTiSe_2,[26] but whether that occurs in Pd_xTiSe_2, where the superconductivity occurs in a much narrower composition range, is not yet known. A quantum critical point may exist in Pd_xTiSe_2 near a critical composition $x_c \approx 0.10$ where the CDW disappears, and future low-temperature study may reveal whether this is indeed the case.

ACKNOWLEDGMENTS

EM acknowledges support from Rice University. Work at Princeton was supported by the U.S. DOE Division of Basic Energy Sciences, Grant No. DE-FG02-96-45702. Work at Brookhaven National Laboratory was supported by the U.S. DOE Division of Basic Energy Sciences under Contract No. DE-AC02-98CH10886.

*emorosan@rice.edu

[1] J. A. Wilson and A. D. Yoffe, Adv. Phys. **18**, 193 (1969).
[2] R. C. Morris, Phys. Rev. Lett. **34**, 1164 (1975).
[3] L. Fang, Y. Wang, P. Y. Zou, L. Tang, Z. Hu, H. Chen, C. Dong, L. Shan, and H. H. Wen, Phys. Rev. B **72**, 014534 (2005).
[4] R. Delaplace, Ph. Molinié, and D. Jérome, J. Phys. (France) Lett. **37**, 13 (1976).
[5] C. Berthier, P. Molinié, and D. Jérome, Solid State Commun. **18**, 1393 (1976).
[6] R. H. Friend, D. Jerome, R. F. Frindttg, A. J. Granttl, and A. D. Yoffe, J. Phys. C **10**, 1013 (1977).
[7] F. J. Di Salvo, D. E. Moncton, and J. V. Waszczak, Phys. Rev. B **14**, 4321 (1976).
[8] J. A. Wilson, Solid State Commun. **22**, 551 (1977).
[9] E. Morosan, H. W. Zandbergen, B. S. Dennis, J. W. G. Bos, Y. Onose, T. Klimczuk, A. P. Ramirez, N. P. Ong, and R. J. Cava, Nat. Phys. **2**, 544 (2006).
[10] R. Z. Bachrach, M. Skibowski, and F. C. Brown, Phys. Rev. Lett. **37**, 40 (1976).
[11] A. Zunger and A. J. Freeman, Phys. Rev. B **17**, 1839 (1978).
[12] C. H. Chen, W. Fabian, F. C. Brown, K. C. Woo, B. Davies, and B. DeLong, Phys. Rev. B **21**, 615 (1980).
[13] G. Margaritondo, C. M. Bertoni, J. H. Weaver, F. Lévy, N. G. Stoffel, and A. D. Katnani, Phys. Rev. B **23**, 3765 (1981).
[14] G. Li, W. Z. Hu, D. Qian, D. Hsieh, M. Z. Hasan, E. Morosan, R. J. Cava, and N. L. Wang, Phys. Rev. Lett. **99**, 027404 (2007).
[15] O. Anderson, R. Manzke, and M. Skibowski, Phys. Rev. Lett. **55**, 2188 (1985).
[16] H. Myron and A. Freeman, Phys. Rev. B **9**, 481 (1974).
[17] N. G. Stoffel, S. D. Kevan, and N. V. Smith, Phys. Rev. B **31**, 8049 (1985).
[18] T. E. Kidd, T. Miller, M. Y. Shou, and T.-C. Chiang, Phys. Rev. Lett. **88**, 226402 (2002).
[19] K. C. Woo, F. C. Brown, W. L. McMillan, R. J. Miller, M. J. Schaffman, and M. P. Sears, Phys. Rev. B **14**, 3242 (1976).
[20] D. Qian, D. Hsieh, L. Wray, E. Morosan, N. L. Wang, Y. Xia, R. J. Cava, and M. Z. Hasan, Phys. Rev. Lett. **98**, 117007 (2007).
[21] N. P. Ong and P. Monceau, Phys. Rev. B **16**, 3443 (1977).
[22] F. J. Di Salvo, B. G. Bagley, J. M. Voorhoeve, and J. V. Waszczak, J. Phys. Chem. Solids **34**, 1357 (1973).
[23] P. Foury, J. P. Pouget, E. Wang, and M. Greenblatt, Europhys. Lett. **16**, 485 (1991).
[24] S. van Smaalen, M. Shaz, L. Palatinus, P. Daniels, F. Galli, G. J. Nieuwenhuys, and J. A. Mydosh, Phys. Rev. B **69**, 014103 (2004).
[25] N. Ru, C. L. Condron, G. Y. Margulis, K. Y. Shin, J. Laverock, S. B. Dugdale, M. F. Toney, and I. R. Fisher, Phys. Rev. B **77**, 035114 (2008).
[26] H. Barath, M. Kim, J. F. Karpus, S. L. Cooper, P. Abbamonte, E. Fradkin, E. Morosan, and R. J. Cava, Phys. Rev. Lett. **100**, 106402 (2008).
[27] K. Mastronardi, D. Young, C. C. Wang, P. Khalifah, R. J. Cava, and A. P. Ramirez, Appl. Phys. Lett. **74**, 1415 (1999).